

Rapid Computational Optimization of Molecular Properties using Genetic Algorithms: Searching Across Millions of Compounds for Organic Photovoltaic Materials

Ilana Y. Kanal,¹ Geoffrey R. Hutchison^{1,2}*

¹Department of Chemistry, University of Pittsburgh, 219 Parkman Avenue,
Pittsburgh, Pennsylvania 15206

²Department of Chemical Engineering, University of Pittsburgh, Pittsburgh, PA 15261

ABSTRACT. Conjugated organic molecules represent an important area of materials chemistry for both fundamental scientific exploration and technological applications. Using a genetic algorithm to computationally screen up to ~25-50 million molecules for organic photovoltaic properties, we find that our methods find top monomers 6,000-8,000 times faster than brute force search. By testing multiple runs and establishing convergence criteria, we show the computational scaling with search space size, common molecular motifs, and discuss the reliability to choose the same molecules independent of initial data set size. We outline remaining areas of difficulty in growing to larger search spaces, potential solutions, and filtering

criteria for potential organic photovoltaic materials. Efficient genetic algorithm searches promise to address a wide range of property-driven inverse design problems in chemistry.

INTRODUCTION.

Computational molecular screening is crucial to many areas of research ranging from drug discovery to discovery of new materials for many industries.¹⁻³ Many methods have so far been used for property-based screening, each of which has virtues and faults. A typical method attractive to many researchers is the development of large libraries of known structures, which can then be searched for molecules of interest for specific applications.^{4,5} Although these libraries take significant computational time to generate, once constructed, they can be repeatedly and easily searched for molecules with particular features. For example, one such study successfully developed a library with small organic molecules for thermally activated delayed fluorescence (TADF).⁵ A similar effort generated a map to search the uncharted areas of the small molecule universe, and targeting molecules that do not yet exist.⁶ Similar libraries can be generated for diverse molecular species with favorable physical property values.⁴

While library generation helps with repeated screening, more typically, researchers are interested in rapidly finding new compounds with particular “best” possible properties – an inverse design problem where the figure of merit is known, but the molecular design motifs are not. New machine learning methods can provide an alternative strategy to generating of large databases. Aspuru-Guzik *et. al.* reported a generative model for efficient searching and optimization through open-ended spaces of chemical compounds. This generative model uses deep neural networks trained on hundreds of thousands of existing chemical structures to construct two coupled functions: an encoder and a decoder with their method being demonstrated for design of drug-like molecules and organic light-emitting diodes.⁷ While neural network

methods allows continuous optimization for molecules, inherently discrete species, so to ensure accurate results, the encoder and decoder functions require a lot of training. Another approach is the use of interpolation of property values, requiring less than 0.01% of the search space to find optimal targets.

While there are many areas of chemistry requiring rapid inverse design of molecules with improved properties, we have focused on π -conjugated organic electronic materials. Using the power of synthetic chemical tailorability, the topic has attracted fundamental scientific understanding on optoelectronic, charge transport, and other properties, as well as a huge range of potential applications.^{8,9} For example, organic photovoltaics employ the donor-acceptor approach in which electron-poor acceptor and electron-rich donor monomers are mixed to create copolymers with the desired optoelectronic properties.¹⁰⁻¹³ Much effort has been made on finding novel monomers or side-chains to tailor the properties of the resulting oligomers and copolymers.¹⁴

In this work, the key question is whether genetic algorithm (GA) screening methods can be made reliable and efficient for performing discrete property-driven optimization of molecules. We have previously focused on GA methods to rapidly find optimal molecular targets for particular properties without pre-generating a library or training set. We seek to grow the search space from ~500,000 compounds,¹⁵ ultimately to ~50 million molecules, by enlarging the pool of potential monomers from 129 to 1759, and sampling all possible sequences.¹⁶⁻¹⁸ While still much smaller than all molecular space ($\sim 10^{60}$),^{19,20} by testing multiple runs and establishing a convergence criteria, we find our methods to be 6,000-8000 times faster than brute force search. We outline remaining areas of difficulty in growing to larger search spaces, potential solutions, and filtering criteria for potential organic photovoltaic materials. The promise of efficient genetic

algorithm sampling of molecular properties can be applied to many other molecular search areas in the future.

COMPUTATIONAL METHODS.

Table 1. Computed ranges of ZINDO HOMO and LUMO eigenvalues for the monomers and homotetramers in each data set indicating the increasing diversity in the search pools with increased number of monomers.

Number of Monomers	Monomer HOMO (eV)		Monomer LUMO (eV)		Tetramer HOMO (eV)		Tetramer LUMO (eV)	
	Min	Max	Min	Max	Min	Max	Min	Max
129	-8.59	-4.17	-3.93	-1.39	-10.33	-5.71	-3.47	+0.58
442	-8.13	-2.70	-5.56	+1.90	-10.39	-4.19	-4.73	+2.86
611	-8.59	-1.29	-4.41	+2.40	-11.32	-3.31	-5.56	+2.92
908	-8.59	-1.22	-4.17	+2.29	-10.66	-3.92	-4.74	+2.45
1235	-8.59	-1.50	-4.41	+2.02	-11.00	-3.25	-4.51	+2.92
1759	-8.59	-2.74	-4.45	+2.40	-11.32	-3.25	-4.73	+2.86

Monomer Data Sets. Five data sets, comprising of 129, 442, 611, 908, 1235 and 1759 monomers, (Tables S1-S41 and Figures S1-S41) were prepared for this study by selecting small monomers that are likely to be used in organic photovoltaics. Monomers were selected from literature reports or obvious synthetic modifications of conjugated monomers, to span a wide range of aromatic and conjugated species. For this study, most of the species studied contain a combination of C, H, N, O, S, F elements, and those containing Si and Se were excluded. In addition, we restricted polymerization sites to those considered most synthetically likely. A range of electron-donating and electron-withdrawing substituents were considered. The monomers span a wide range of electronic properties as shown in Table 1, with highest occupied molecular

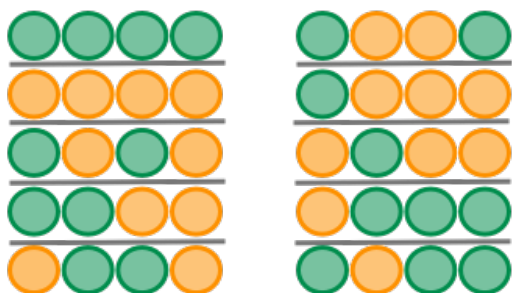
orbital (HOMO) and lowest unoccupied molecular orbital (LUMO) eigenvalues displaying a several electron-volt span for each data set. For comparison, thiophene is computed to have a HOMO eigenvalue of -8.54 eV and a LUMO at -2.03 eV.

Generation of Optimized 3D Structures. The 3D structure of a homotetramer was generated using a multistep process starting with the SMILES string for the polymer.²¹ An initial 3D structure was generated using Open Babel 2.4.0²² (accessed through its Python interface Pybel)²³ and minimized using the MMFF94 force field (500 steps using steepest descent minimization, convergence at 1.0^{-4} kcal/mol). Next a weighted-rotor search (MMFF94, 100 iterations, 20 geometry optimization steps) was carried out to find a low-energy conformer. This was then further optimized using MMFF94 (500 steps). Finally, Gaussian 09²⁴ was used to optimize the structure using the PM6 semiempirical method.²⁵ The entire procedure required ~8 min per oligomer on one CPU core.

Prediction of Electronic Structure and Optical Excitation Energies. The energies and oscillator strengths of the 15 lowest-energy electronic transitions were calculated from the PM6-optimized geometry²⁵ using the ZINDO/S method²⁶ as implemented in Gaussian09.²⁴ The Python library `cclib`²⁷ was used to extract the molecular orbital eigenvalues, energies and oscillator strengths of the electronic transitions. The accuracy of this method was tested in our previous work¹⁵ and was shown to be sufficient.²⁸

Synthetic Accessibility. To limit the possible search space and to concentrate on the most synthetically relevant species, we considered copolymers formed by preparing a dimer of two

different monomers, followed by polymerization to make tetramers of all possible sequences (as illustrated in Scheme 1) generating 264,192 tetramers (129 monomer set), 3,118,752 tetramers (442 monomer set), 5,963,360 tetramers (611 monomer set), 13,176,869 tetramers (908 monomer set), 24,383,840 tetramers (1235 monomer set) and 49,477,152 tetramers (1759 monomer set). In addition, hexamers were tested for the data sets containing 129, 442 and 908 monomers, increasing the number of molecules screened to over 52 million compounds.



Scheme 1. Tetramer sequences permitted within the genetic algorithm for the combination of two monomers.

Calculation of Energy Conversion Efficiency. As with our previous work, the predicted power conversion efficiency was calculated as described by Scharber *et al.*²⁹ on the basis of the orbital energy levels and first excitation energy of the oligomer/polymer donor material relative to (PCBM). Our implementation is identical to previous work¹⁵ and details can be found in the supporting information.

Genetic Algorithm. A genetic algorithm (GA) is a stochastic method for global optimization based on concepts from evolution, in which a population of chromosomes is optimized in successive generations by applying the evolutionary operators of crossover, mutation and

selection. In our study, the chromosomes were the candidate co-oligomers, and successive generations minimized the deviation from the HOMO and electronic transition energy values at the point of maximum efficiency.

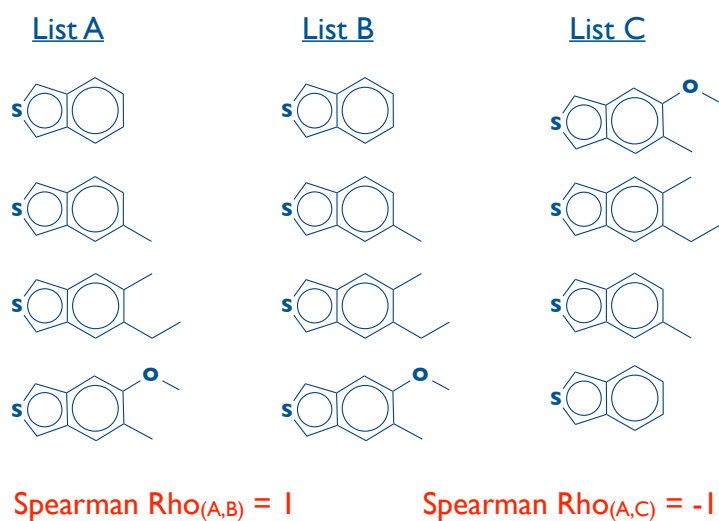
A key feature of our genetic algorithm implementation was the mutation operator allowing for mutation between monomers with similar electronic properties. To define “similar,” for each of the monomers we generated 3D structures (as described above) of the corresponding homooligomer of length 4 and carried out a ZINDO/S single-point calculation. Similar monomers were defined as those oligomers with similar HOMO and LUMO eigenvalues, as measured by 2D Euclidean distance. Full details of the genetic algorithm are available in the Supporting Information.

Analysis. Results from the genetic algorithm were analyzed using Python with `numpy`³⁰ and `pandas`³¹ modules to generate histograms of monomers most often chosen and determine Spearman correlations and the percentage of monomers which were identical in different data sets to identify the top monomers and the number of generations needed for the convergence of the set of top monomers.

RESULTS AND DISCUSSION.

Scaling of our GA to massive search spaces. Determining the number of generations required to converge the list of top performing molecules is essential to scaling a genetic algorithm to large search spaces. Ideally, data from several runs, with different initial populations, can provide a set of monomers in which the most frequently chosen monomers are identical in each set. Data set convergence to these sets of top monomers was determined

through calculation of the Spearman rank correlation that quantifies how well two lists are described with a monotonic function when ranked in order of energy. Two identically ordered lists produce a perfect Spearman correlation of +1, and an inversely ordered list provides a perfectly inverse Spearman correlation of -1. (**Scheme 2**)



Scheme 2. Spearman rank correlation explained. Two identically ordered lists have a Spearman correlation of +1, while two lists which are ordered exactly opposite of each other have a Spearman correlation of -1.

For each of the five data sets described in the computational methods section, Spearman correlations (ρ) were calculated at intervals within the range of 1-100 generations. Convergence of each data set to a set of top monomers was approximated at the value where the average Spearman correlation is equal to 0.50. This cutoff was chosen due to the logarithmic scaling exhibited by the data, and therefore it would be necessary to calculate vastly more generations to achieve greater correlation. An analysis of this threshold value is performed below. Equations of

best fit for the top 5, 10, 15, 20 and 25% of the data were determined and used to calculate the number of generations required to achieve data set convergence (Figures S42-43, Tables 42-45).

Table 2. The number of calculated generations to convergence of the top monomers for the top X% of the tetramer data. Convergence was calculated using the equations of fit to exceed 0.5 correlation.

Number of Monomers	25%	20%	15%	10%
129	9.2 ± 1.1	8.4 ± 1.1	7.27 ± 0.93	6.76 ± 1.1
442	14.2 ± 2.6	11.7 ± 2.0	10.57 ± 1.94	10.4 ± 2.2
611	16.7 ± 2.0	20.4 ± 2.2	33.16 ± 2.77	Does not converge
908	41.2 ± 2.5	51.3 ± 3.6	59.99 ± 5.72	61.76 ± 6.6
1235	48.6 ± 4.3	60.7 ± 5.2	80.38 ± 5.26	97.42 ± 3.8
1759	Does not converge			

The results for the number of generations to convergence are summarized in Table 2 and show that as the data set increases in magnitude, the number of generations needed for the convergence of the top monomer set also increases only modestly. For completeness, the top 25% of the hexamer data was analyzed and results corroborated the tetramer data: the 129 monomers set converges in 5.99 ± 0.98 generations, the 442 monomer set converges in 12.86 ± 1.52 generations and the 908 monomer set converges in 57.15 ± 10.7 generations. These values are within error of the tetramer values showing that the data set is effectively being screened. Using the number of generations required for each of the different sized data sets to achieve to convergence, it is possible predict the number of generations to convergence for data sets of different sizes (Figure 1).

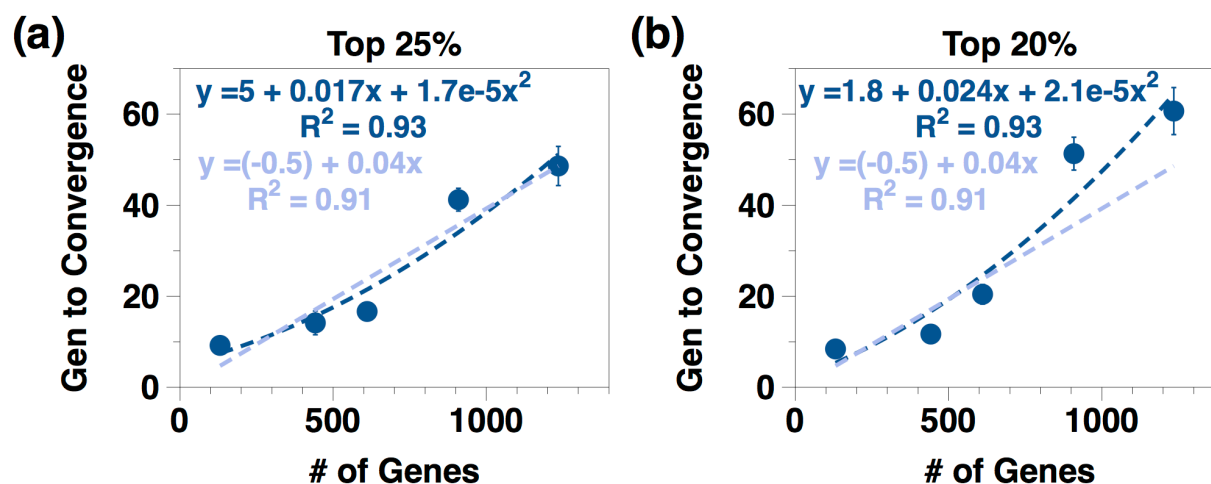


Figure 1. Number of generations required for top monomer convergence for different sized data sets. For both (a) the top 20% and (b) the top 25% data sets, the number of generations required for data set convergence is quadratic or linear excluding the 1759 monomer data set which did not achieve convergence.

For data sets smaller than 1235 monomers, the model is slightly quadratic or possibly linear, but at larger values (i.e., 1759) the data does not converge to a set of top monomers since the search space is evidently too large. The data sets examining the top 25% and 20% both show R^2 values for the quadratic fit of 0.93 for the prediction of the number of generations required to achieve convergence of a data set and R^2 values for the linear fit of 0.91, excluding the point for 1759 monomers.

The error in the number of generations to convergence, as reported in Table 2 was determined by taking the residual from the line of best fit divided by the square root of the sample size. The number of generations to convergence was then calculated for $0.5 \pm$ this value and the error was determined by subtracting the two new values for the generations to convergence. Unsurprisingly, as the data set increases in size, the error in the number of

generations to convergence also increases since more space to sample, with all other parameters remaining constant, and therefore not efficiently sampling the entire data set, as completely as in smaller data sets.

Efficiency of our GA approach. The discrepancy in the number of generations to convergence with 1235 and 1759 monomers demonstrates that a region exists in which the number of monomers in a data set have maximum efficiency. Each generation in our screening consists of 64 calculations (one for each “chromosome”). The fraction of the calculations which we must perform to achieve convergence for a data set of a particular size is the number of calculations to convergence (i.e., 64 calculations per generation times the number of generations to convergence) divided by the number of calculations in an exhaustive search for that data set. The speedup is therefore the reciprocal of this value or the number of calculations in an exhaustive search divided by the number of calculations to convergence (Tables S46-47).

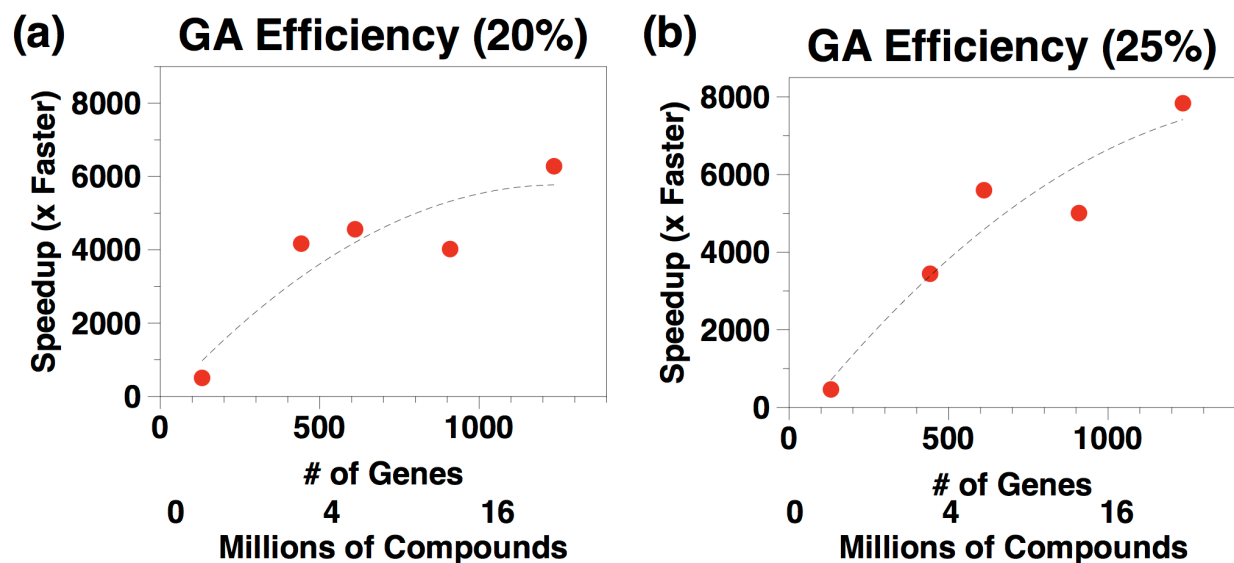


Figure 2. The speedup as calculated from the number of calculations performed when running the genetic algorithm compared with the number of calculations required for an exhaustive search. As shown in (a) top 20% and (b) top 25%.

While the “easiest” solution to screening millions of molecules would seem to be to screen through an exhaustive search where calculations are performed for each molecule, in reality this is a very slow and therefore costly approach. As illustrated in Figure 2, our GA converges to a set of top monomers with a speedup of $\sim 6000x$ over brute force (for 1235 monomers across the top 20%), and a speedup of $\sim 8000x$ (for 1235 monomers across the top 25%). Since the largest search space did not converge, for future screening of large data sets, a tournament style approach would likely improve efficiency with increasingly large groups. In a tournament approach, the initial monomer pool would be divided into several optimally sized groups ($\sim 1,000$ monomers each). Each group can be screened for top monomers and then the top monomers can compete against one another to determine the overall top monomers.

Properties of Top Candidates

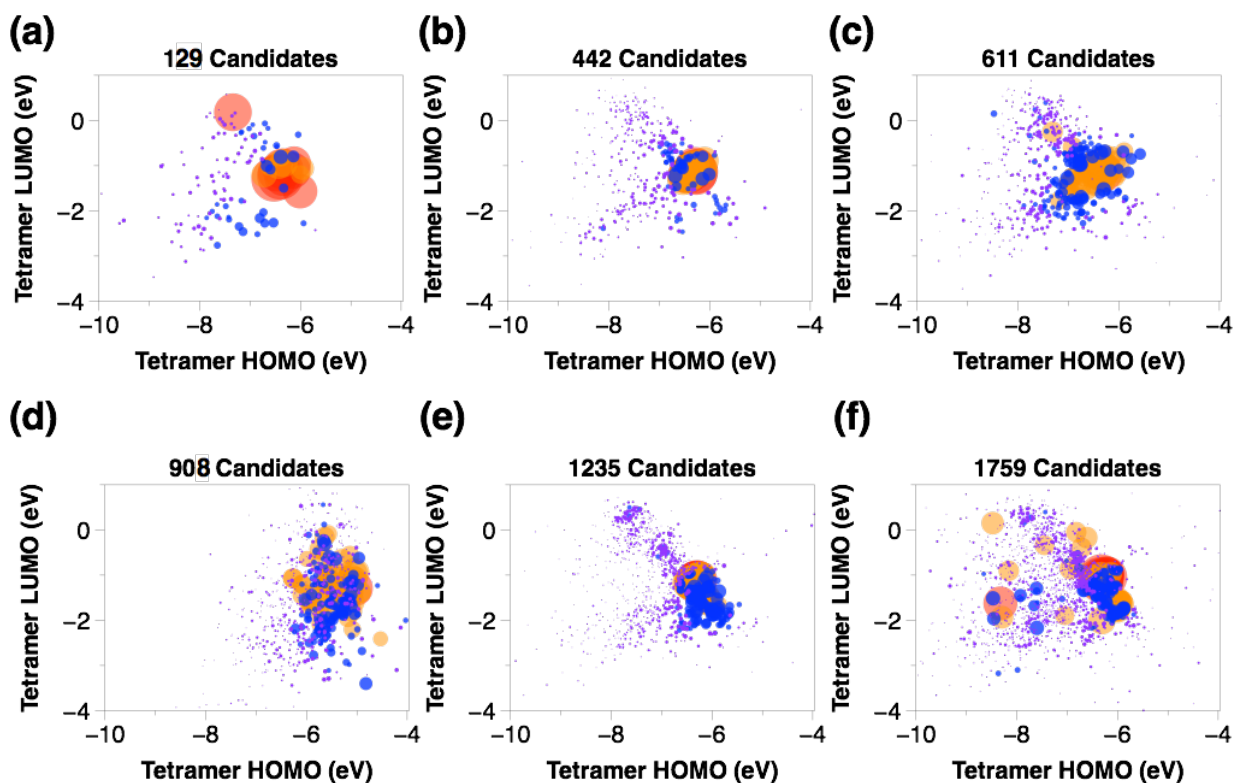


Figure 3. “Hotspots” of homotetramer HOMO and LUMO data (after 100 generations), with size and color of the spot normalized based on the frequency of occurrence of each monomer, indicates that in all data sets, tetramers with HOMO energies ranging from -9 to -5 eV and LUMO energies in the range of -3 to +1 eV show promise as candidates for solar cells. This can be used to prescreen candidates in future experiments to eliminate candidates with energies far outside this range.

Initial random selection of monomers yield a diverse population of HOMO and LUMO energies after the first generation in each set of data, independent of the size of the data set. However, as the GA proceeds through multiple generations, HOMO and LUMO energies which

are selected in the remaining population of monomers narrows to a “hot spot” that emerges within each group of data. These hotspots emerge as the number of generations approaches the number of generations at which the data set converges. In each of the data sets studied, tetramers with HOMO energies ranging from -9 to -5 eV and LUMO energies in the range of -3 to +1 eV are selected with high frequency as candidate materials for solar cells. The existence of an energy “hot spot” can be used to prescreen candidates in future experiments to eliminate tetramers with energies far outside this range and thus excluding them from the similarity matrix. This would enable more thorough screening of larger data sets in fewer generations as some molecules are eliminated before the GA begins working on the selected data.

Additional Predictive Properties. Homotetramer HOMO and LUMO energies have significant impact on the species selected by the GA. This can allow for eliminating molecules with energies significantly outside these thresholds. To further improve the GA, it would be beneficial to identify other predictive properties that can reliably remove uninteresting molecules and focus toward useful candidate molecules. A stepwise regression was performed to determine properties which effect the frequency with which a molecule is chosen and included properties such as tetramer HOMO, tetramer LUMO, tetramer excitation energy, tetramer oscillation strength, monomer HOMO and monomer LUMO. For each data set, the parameters selected that control the frequency of monomer selection are tetramer HOMO and tetramer LUMO, which are already used in the GA. Interestingly, an additional parameter of the tetramer excitation energy effects the frequency in each of the data sets examined. A random forest analysis corroborated this finding. In future work, generation of the similarity matrix, will include the tetramer HOMO, tetramer LUMO and tetramer excitation energy, leading the similarity matrix to be a better predictor of the ideal materials and provide top monomer convergence in fewer generations.

Top Monomers from the GA. While the determination of the most likely monomer candidates for solar applications is the goal of running this genetic algorithm, deciding how to define this group of top monomers was not straight forward. In our previous work with 129 monomers, we were able to analyze the top 25 monomers. When comparing sets of data with substantially different numbers of monomer, we realized that examining the top X% of the data set was a more meaningful comparison since most of the data comes from a small subset of the monomers as shown by the histograms in Figure S44. To determine which percentages to examine, the number of monomers which comprise 25%, 50%, 75%, 80%, 90%, 95%, 98% and 99% were examined and converted to percentages of the total data for comparison between different sized data sets. The results from this are reported in Table 3, and show that up to 90% of the data comes from a small percentage of the total number of monomers. We therefore analyze the top 10% and the top 20% of the monomers as these data sets contain most of the data from a given run of the GA.

Table 3. Analysis of the percentage of monomers which comprise different percentages of data reveals that up to 90% of the final data comes from a small fraction of the initial data set.

Percentage of Top Candidates	Fraction of monomers that comprise top X% of candidates after 100 generations					
	129	442	611	908	1235	1759
25%	2%	1%	2%	1%	1%	1%
50%	5%	3%	2%	4%	3%	2%
75%	8%	5%	12%	6%	6%	5%
80%	10%	6%	14%	7%	7%	5%
85%	12%	7%	17%	9%	9%	6%
90%	18%	10%	23%	11%	11%	8%
95%	34%	23%	36%	27%	19%	16%

Analysis to determine the top monomers in the top 10% and top 20% of the data set and whether there is overlap in the top data sets unaffected by the starting pool of monomers was performed on the percentage of the original data set, rounded up to whole numbers. The number of monomers for the top 10% analysis was 14 (129 monomer set), 45 (442 monomer set), 62 (611 monomer set), 91 (908 monomer set), 124 (1235 monomer set) and 176 (1759 monomer set). Likewise, the number of monomers for the top 20% analysis was 27 (129 monomer set), 89 (442 monomer set), 123 (611 monomer set), 182 (908 monomer set), 247 (1235 monomer set) and 352 (1759 monomer set). Analysis was performed on the data after 100 generations and after the number of generations calculated for each size data set to converge to a set of top monomers and these calculations both yield similar results reinforcing our calculations which predict the results of the number of generations to reach a set of top monomers. Table 4 presents the number of monomers from each smaller group of data that overlap with the larger data sets, in a pairwise analysis after 100 generations in each case. In both analysis of both the top 10% and 20% of the candidate molecules, an overwhelming number of monomers from the smaller pool of candidates

appear in the larger sets of data, even through multiple runs each starting with a different random seed of candidates from the given data set. Building on the finding that there is significant overlap in the pairwise analysis of the different sized data sets, we questioned whether there are a group of candidate molecules which appear in the top 10% and the top 20% of *all* data sets examined in this study.

Table 4. Overlap analysis of the pairwise combination of the data for the top 10% and top 20% of the candidates reveals that most of the candidates that are chosen in the smallest data group (129) are still chosen as important candidates when the monomer pool is increased by more than 10-fold.

	Top 10% of Candidates						Top 20% of Candidates					
	129	442	611	908	1235	1759	129	442	611	908	1235	1759
129		85%	64%	79%	64%	71%		59%	52%	48%	52%	59%
442			70%	67%	60%	60%			62%	56%	54%	54%
611				47%	42%	40%				36%	40%	39%
908					33%	48%					31%	59%
1235						75%						65%

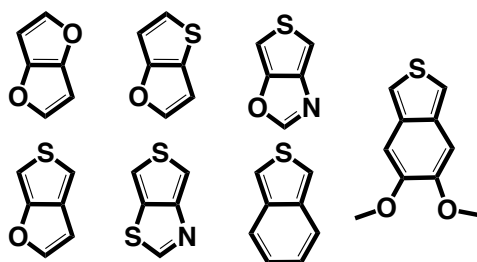


Figure 4. The top seven monomers which appear across *all* data sets for the top 10% and top 20% of the data.

Figure 4 illustrates the seven monomers that are present in *all* data sets in both the top 10% and the top 20% of the data. While only three of these species have been synthesized to our knowledge, all seven have previously been cited in papers or patents as potential materials for improved OPV materials. While some may be challenging to synthesize, the retained bi-aromatic ring structure is clearly an important motif, and the presence of hotspots in Figure 3, indicate related analogues with greater synthetic accessibility are likely. We note that none of the top seven monomers are typical electron-poor acceptor motifs, suggesting limits to the conventional donor-acceptor strategy ubiquitous in organic photovoltaic materials.

Sequence Analysis. As with the top monomer analysis, we examined the sequences chosen for each of the monomer pairs selected by the GA to determine if the GA can select a method to combine two monomers in a more favorable manner to generate more efficient materials for solar energy. After examining all the data sets, we determine that each of the sequences is chosen about equally except for AAAA which is surprisingly chosen ~10 times more often compared with the other possible sequences. Calculations of three data sets with hexamers (129, 442 and 908) indicate that the same bias exists with hexamers. In future experiments, adjusting the algorithm to place more importance on the sequence selection may help further screen materials. Interestingly, despite the ubiquitous use of copolymers in experimental investigation of organic electronics, the GA indicates selected homopolymers may still have interesting properties.

Top Monomer Pairs.

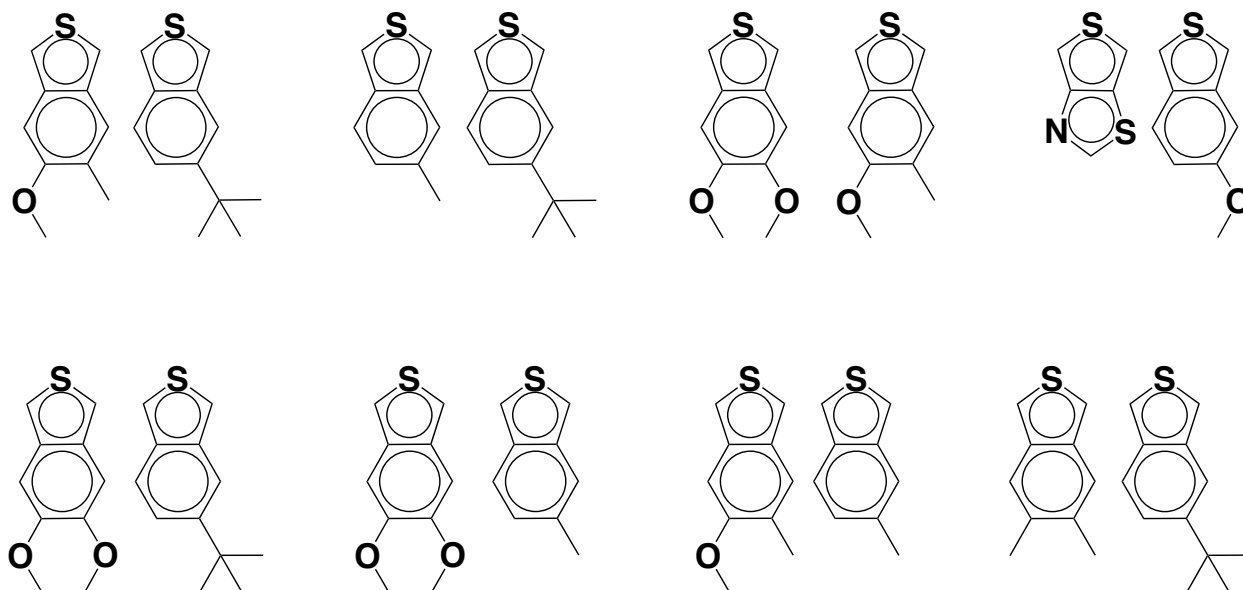


Figure 5. Monomer pairs from tetramer GA runs with 442, 611, 908, 1235 and 1759 candidates after 100 generations revealed that the same pairs are chosen most often regardless of size of data set.

In addition to analysis of top monomers chosen, selected monomer pairs were also examined. In each step of the GA, two monomers are chosen to form a co-oligomer and therefore, it is logical to look at the pairs with the top performance and frequency. Data was examined after 100 generations for each of the tetramer runs by selecting each of the two monomers, ensuring a unique combination (e.g., AB = BA) and then counting the frequency of each pair. Figure 5 illustrates the eight monomer pairs that were selected most often across the 442, 611, 908, 1235 and 1759 data sets. The set of data with 129 candidates is excluded from this analysis, since some of the monomers were not present in this smaller set. This data is corroborated with the hexamers from the 442 and 908 runs which show the same set of top monomers. Clearly the

isobenzothiophene, a known low-band gap system, is an influential motif, particularly when combined with electron-donating substituents such as alkyl or alkoxy functional groups.

CONCLUSIONS

Genetic algorithm methods are known as efficient techniques for optimizing discrete variables, such as molecular structures. This work shows that, when selecting conjugated oligomers, the GA approach is ~6000-800 times faster than brute force. Since the GA is independent of computational methods used, it can provide rapid filtering of lead compounds using first principles, semiempirical, or machine learning methods alike. Moreover, we find only modest scaling of the number of generations required to converge the set of top candidates up to a search space of ~25 million compounds.

Unfortunately, convergence, as judged by the Spearman rank correlation of the top candidates, is not found for a larger search space. Instead, the GA appears stuck in local regions and cannot explore the entire (vast) search space. In future work, we believe a divide-and-conquer approach that partitions large searches into smaller regions, combined with a competition among top candidates will address this problem.

Moreover, we find all searches, regions of “hot spots” (Figure 3) which comprise monomers frequently incorporated in top candidates. This suggests broader searches can perform some level of initial filtering based on these properties. That is, a new monomer found far from a hotspot is unlikely to be among top candidates and can likely be ignored. Predicting the frequency of monomer genes among top candidates will clearly improve the efficiency of the GA search – the presence of such hotspots suggests that for organic electronic materials, statistical and machine learning approaches can rapidly identify interesting new leads.

Molecular space is known to be enormous, but the application of efficient GA search techniques offers great promise for finding optimal and near-optimal targets for a wide range of computationally-driven properties. The techniques outlined here for organic electronic materials can easily be adopted for many other electronic structure properties, from redox potentials and activation energies, to polarity, polarizability and dielectric constants.

Supporting Information. The following files are available free of charge.

brief description (file type, i.e., PDF)

Corresponding Author

* geoffh@pitt.edu

ACKNOWLEDGMENT We thank the University of Pittsburgh, including the Center for Energy for support, and NSF (CBET-1404591). GRH thanks Dr. Noel O’Boyle and Prof. Tara Meyer for discussions.

REFERENCES

- 1 S. P. Ong, W. D. Richards, A. Jain, G. Hautier, M. Kocher, S. Cholia, D. Gunter, V. L. Chevrier, K. A. Persson and G. Ceder, *Computational Materials Science*, 2013, **68**, 314–319.
- 2 G. Montavon, M. Rupp, V. Gobre, A. Vazquez-Mayagoitia, K. Hansen, A. Tkatchenko, K.-R. Müller and O. A. Von Lilienfeld, 2013.
- 3 I. E. Castelli, T. Olsen, S. Datta, D. D. Landis, S. Dahl, K. S. Thygesen and K. W. Jacobsen, *ENERGY & ENVIRONMENTAL SCIENCE*, 2012, **5**, 5814–5819.
- 4 C. Rupakheti, A. Virshup, W. Yang and D. N. Beratan, *J Chem Inf Model*, 2015, **55**, 529–537.
- 5 C. Rupakheti, R. Al-Saadon, Y. Zhang, A. M. Virshup, P. Zhang, W. Yang and D. N. Beratan, *J Chem Theory Comput*, 2016, **12**, 1942–1952.

- 6 A. M. Virshup, J. Contreras-García, P. Wipf, W. Yang and D. N. Beratan, *J Am Chem Soc*, 2013, **135**, 7296–7303.
- 7 R. Gómez-Bombarelli, D. Duvenaud, J. M. Hernández-Lobato, J. Aguilera-Iparraguirre, T. D. Hirzel, R. P. Adams and A. Aspuru-Guzik, 2016.
- 8 C. Wang, H. Dong, W. Hu, Y. Liu and D. Zhu.
- 9 T. M. Swager, *Macromolecules*, 2017, acs.macromol.7b00582.
- 10 A. Facchetti, *Chem. Mat.*, 2011, **23**, 733–758.
- 11 J. M. Szarko, J. Guo, B. S. Rolczynski and L. X. Chen, *J Mater Chem*, 2011.
- 12 X. Zhao and X. Zhan, *Chem. Soc. Rev.*, 2011, **40**, 3728–3743.
- 13 C. Risko, M. D. McGehee and J.-L. Brédas, *Chem. Sci.*, 2011, **110**, 59–69.
- 14 J. Mei and Z. Bao, *Chem. Mater.*, 2014, **26**, 604–615.
- 15 N. M. O'Boyle, C. M. Campbell and G. Hutchison, *J Phys Chem C*, 2011, **115**, 16200–16210.
- 16 S. Zhang, N. E. Bauer, I. Y. Kanal, W. You, G. R. Hutchison and T. Y. Meyer, *Macromolecules*, 2017, **50**, 151–161.
- 17 B. N. Norris, S. Zhang, C. M. Campbell, J. T. Auletta, P. Calvo-Marzal, G. Hutchison and T. Y. Meyer, *Macromolecules*, 2013, **46**, 1384–1392.
- 18 J. Li, R. M. Stayshich and T. Y. Meyer, *J Am Chem Soc*, 2011, **133**, 6910–6913.
- 19 R. van Deursen and J.-L. Reymond, *ChemMedChem*, 2007, **2**, 636–640.
- 20 T. Fink, H. Bruggesser and J.-L. Reymond, *Angew Chem Int Edit*, 2005, **44**, 1504–1508.
- 21 D. Weininger, *J. Chem. Inf. Comput. Sci.*, 1988, **28**, 31–36.
- 22 N. M. O'Boyle, M. Banck, C. A. James, C. Morley, T. Vandermeersch and G. Hutchison, *J. Cheminf.*, 2011, **3**, 33.
- 23 N. O'Boyle, C. Morley and G. Hutchison, *Chemistry Central Journal 2008 2:24*, 2008, **2**, 5.
- 24 M. J. Frisch, G. W. Trucks, H. B. Schlegel, G. E. Scuseria, M. A. Robb, J. R. Cheeseman, G. Scalmani, V. Barone, G. A. Petersson, H. Nakatsuji, X. Li, M. Caricato, A. V. Marenich, J. Bloino, B. G. Janesko, R. Gomperts, B. Mennucci, H. P. Hratchian, J. V. Ortiz, A. F. Izmaylov, J. L. Sonnenberg, Williams, F. Ding, F. Lipparini, F. Egidi, J. Goings, B. Peng, A. Petrone, T. Henderson, D. Ranasinghe, V. G. Zakrzewski, J. Gao, N. Rega, G. Zheng, W. Liang, M. Hada, M. Ehara, K. Toyota, R. Fukuda, J. Hasegawa, M. Ishida, T. Nakajima, Y. Honda, O. Kitao, H. Nakai, T. Vreven, K. Throssell, J. A. Montgomery Jr, J. E. Peralta, F. Ogliaro, M. J. Bearpark, J. J. Heyd, E. N. Brothers, K. N. Kudin, V. N. Staroverov, T. A. Keith, R. Kobayashi, J. Normand, K. Raghavachari, A. P. Rendell, J. C. Burant, S. S. Iyengar, J. Tomasi, M. Cossi, J. M. Millam, M. Klene, C. Adamo, R. Cammi, J. W. Ochterski, R. L. Martin, K. Morokuma, O. Farkas, J. B. Foresman and D. J. Fox, 2009.
- 25 J. J. P. Stewart, *J. Mol. Model.*, 2007, **13**, 1173–1213.
- 26 J. Ridley and M. Zerner, *Theoret. Chim. Acta*, 1973, **32**, 111–134.
- 27 N. M. O'Boyle, A. L. Tenderholt and K. M. Langner, *J. Comp. Chem.*, 2008, **29**, 839–845.
- 28 G. Hutchison, M. A. Ratner and T. J. Marks, *J Phys Chem A*, 2002, **106**, 10596–10605.
- 29 M. Scharber, D. Wuhlbacher, M. Koppe, P. Denk, C. Waldauf, A. J. Heeger and C. J. Brabec, *Adv. Mater.*, 2006, **18**, 789–.
- 30 S. Walt, S. C. Colbert and G. Varoquaux, *Computing in Science & ...*, 2011.
- 31 W. McKinney, 2010, 51–56.